

Study on the Safety Factors of the Bedding Rock Slope under Dynamic Loading

Liu Xinrong^{1,2}, He Chunmei^{1,2,*}, Li Xingwang^{1,2}, Liu Gang³ and Zeng Bin⁴

¹School of Civil Engineering, Chongqing University, Chongqing 400045, China

²Key Laboratory of New Technology for Construction of Cities in Mountain Area (Chongqing University), Ministry of Education, Chongqing 400045, China

³Sinohydro Bureau 14 Co., Ltd, Kunming 650041, China

⁴School of Civil, Environmental and Mining Engineering, The University of Western Australia, Crawley, WA 6009, Australia

Received 19 April 2016; Accepted 25 June 2016

Abstract

Analysis of a bedding rock slope model with a structural surface that connects a splay fracture and penetrates through the slope was conducted based on the strength reduction method to study the dynamic response and deformation process of a rock slope-containing surface. The critical state of the bedding rock slope was estimated using the trend of the key point displacement time history curve. The safety factor and sliding surface were also estimated by the displacement vector diagram of the instable slope. The calculated results were verified by obtaining the safety factor and sliding surface through the displacement vector diagram method used in this paper and comparing them with those obtained using the limit equilibrium method. A preliminary analysis on the effects of the slope height, slope gradient, and bedding inclination on the safety factors of the bedding rock slope under dynamic loading was conducted with the finite difference analysis software, FLAC^{3D}. Results showed a slight difference between the safety factors of the two different methods, and the sliding surface was consistent with one another in the location, indicating that the method used in this paper was appropriate. The dynamic safety factors of the bedding rock slope gradually decreased with the increase of slope height, significantly decreased with the increase of bedding inclination, and began to stabilize after a dramatic decrease with the increase of slope gradient. Findings offer solid guidance for time-history analysis on the dynamic stability of the rock slope encountering severe earthquakes and long-term stability analysis of the bedding rock slope under dynamic loading.

Keywords: Bedding rock slope, Strength reduction method, Finite difference method, Dynamic loading, Safety factors

1. Introduction

Rock slopes are prevalent in transportation construction, water conservancy and hydropower, mining, civil engineering, and other fields. Its destruction and instability are major issues that affect or constrain engineering construction. For instance, the Three Gorges reservoir area has numerous bedding rock slopes, which seriously affect the safety of the construction and operation of infrastructure in the area, such as roads and railways, because of poor stability. Rock slopes are generally stable under the natural state. However, rock slopes under dynamic loading often lead to landslides and collapses. Earthquake-induced landslides, which are different from static-induced landslides, lead to more serious disasters [1], [2].

Therefore, based on FLAC^{3D}, revealing the mechanism of slope instability and reasonably evaluating the slope-containing surface under dynamic loading are highly significant in studying the dynamic response and deformation process, obtaining the critical sliding surface of layered rock slope and its corresponding safety factor, and simulating the expanding law of plastic zones and the final failure mode.

2. State of the art

The methods to calculate the slope seismic stability include pseudo-static analysis, Newmark sliding block analysis, numerical simulation analysis, and so on [3]. Pseudo-static analysis is widely applied because it can simplify the dynamic slope stability analysis [4], [5], [6], [7]. However, this method cannot reflect the dynamic characteristics of dynamic loading because it takes the dynamic loading as static load. Meanwhile, Newmark sliding block analysis is a method used to evaluate the slope stability according to the seismic permanent deformation, which is essentially an average displacement and cannot reflect the displacement distribution of each point in the rock slope under earthquake loading [8]. Therefore, Newmark sliding block analysis is still unable to evaluate slope stability. Numerical simulation analysis, which contains the discrete element method [9], finite difference method [10], [11], and so on, can effectively obtain the numerical solution of mechanical response and the corresponding time-history curves. Although the numerical solution is an approximation, calculation results using a reasonable calculation model can meet the precision that engineering requires. R. Bhasin et al. studied both the static and dynamic simulations of a 700-m high slope to predict the failure characteristics under earthquake loading by using a two-dimensional discrete element program of Universal Distinct Element Code (UDEC) [12]. Teng G L et al. studied the effects of slope

* E-mail address: hechunmei0427@126.com

ISSN: 1791-2377 © 2016 Eastern Macedonia and Thrace Institute of Technology.
All rights reserved.

height, seismic intensity, slope angle, and joint inclination combination on the jointed rock slope stability by establishing an ideal two-dimensional discrete element model [13]. Facciorusso J et al. put forward a grade-3 method of zonation for seismic slope stability [14]. With respect to numerical simulation studies, the finite element method is used mainly to analyze the dynamic safety factors and long-term stability of the slope under dynamic loading. Thus, using the finite difference method as the research method is less.

The remainder of this paper is organized as follows. Section 3 introduced the research method. Section 4 simulated two cases. Case 1 calculated a bedding rock slope model with a structural surface that connects a splay fracture and penetrates through the slope using two methods. One of the methods was the displacement vector diagram method used in this paper, and the other one was the limit equilibrium method. Furthermore, the calculated results were compared with each other to validate whether the method used in this paper was feasible. Moreover, Case 2 analyzed the effects of different slope height, slope gradient and bedding inclination influences on the safety factors under dynamic loading by calculating a bedding rock slope model with a group of beddings. Conclusions are summarized in Section 5.

3. Methodology

3.1 Strength reduction method

The strength reduction method is essentially a search algorithm, in which the actual shear strength of the slope is divided by the strength reduction factor. The strength reduction factor is adjusted continuously to decrease the rock strength until the slope reaches its critical balance state. The reduction factor w_{cr} in the critical state is defined as the safety factor of the slope [15].

The corresponding equations are as follows:

$$c' = \frac{c}{w} \quad (1)$$

$$\phi' = \tan^{-1} \frac{\tan \phi}{w} \quad (2)$$

$$F_s = w_{cr} \quad (3)$$

where

c, ϕ stand for the actual cohesion and internal friction angle of the ground, respectively;

c', ϕ' refer to the reduced cohesion and internal friction angle, respectively; and ,

F_s represents the slope safety factor.

A. Locat et al. theoretically and experimentally verified the strength of slope sliding zones, which were formed gradually in the process decrease from the peak strength to residual strength [16], [17]. Thus, the reduction of geotechnical materials should be taken into account when considering the slope stability analysis.

3.2 Critical state determining

The essential factor in dynamic strength reduction method is on how to determine whether the slope reaches the critical state. Under static loading, three criteria types are used mainly for the critical state of slopes: (1) the stress distribution of the slope mass, such as the existence of the continuous plastic zone or equivalent plastic strain from the slope toe to the slope top; (2) the deformation characteristics of the slope mass, such as sudden changes in the strain and key point displacement or the sliding surface; and, (3) the convergence of the numerical calculation. For the dynamic strength reduction method, no such convergence exists for the calculation because of the constantly changing real-time stress, deformation, and other parameters. Thus, the deformation characteristic of the slope body is used mostly as the criterion by the researcher in the dynamic strength reduction method. For convenience in studying the dynamic stability of the bedding rock slope under the effects of the earthquake, the time-history curve convergence of the key point displacement is used as the criterion, based on which the dynamic safety factor of the slope is calculated.

In the analysis of the dynamic slope safety factor with such criterion, the simulation based on the finite element method is mostly used, with lesser studies on the dynamic safety factor of the slope under dynamic loading using the finite difference method.

4. Result Analysis and Discussion

4.1 Case 1

A rock slope model with a structural surface that connects a splay fracture and penetrates through the slope is established in the finite difference analysis software, FLAC^{3D}, and its safety factor calculation under dynamic loading is used as an example to demonstrate the displacement vector diagram method. The model length is 500 m and the model height is 200 m. The slope height is 100 m, with a bedding inclination angle of 30° and a slope angle of 60°. The simulation model is shown in Fig. 1. The physical and mechanical properties of the rock layer and structural planes are shown in Tables 1 and 2, respectively. Because the micro seismic waves usually occur with relatively low earthquake magnitude and last shortly (often for 5 to 10 seconds), the modified time-history curve of the earthquake acceleration velocity from a real earthquake record is used for the analysis. The part of the original curve that belongs to the foreshock period is skipped and the wave band from 26 to 33 seconds, lasting for a total of 7 seconds, is used as the wave form of the seismic wave (see Fig. 2). The time-history curve of the earthquake wave is reduced to earthquake intensity IV (with a maximum acceleration speed of 0.22 m/s²), and then used as the time-history curve of the acceleration speed in the FLAC^{3D} calculation. In the simulation, the rock mass is elastic-plastic. The Mohr-Coulomb yield criterion is adopted and the Coulomb's sliding model with the surface contact is used for the structural plane. The boundary is defined as viscous with local damping, with a damping coefficient of 0.15[18].

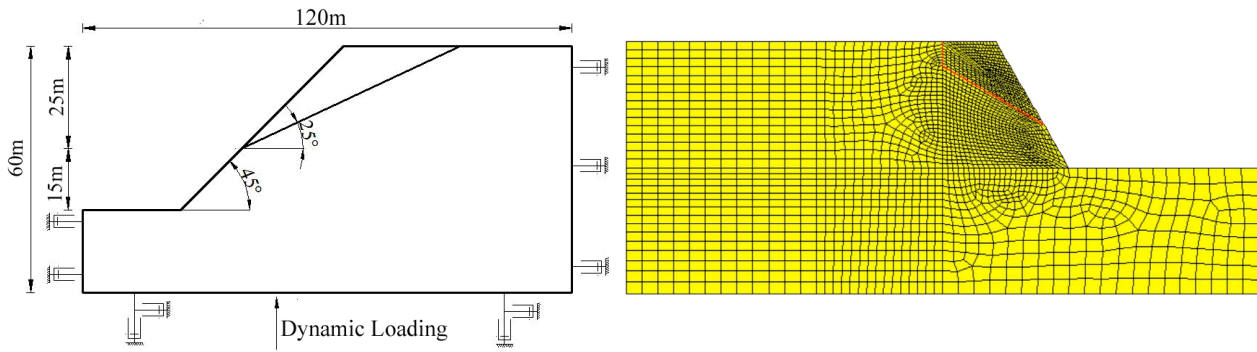


Fig.1. Analysis model

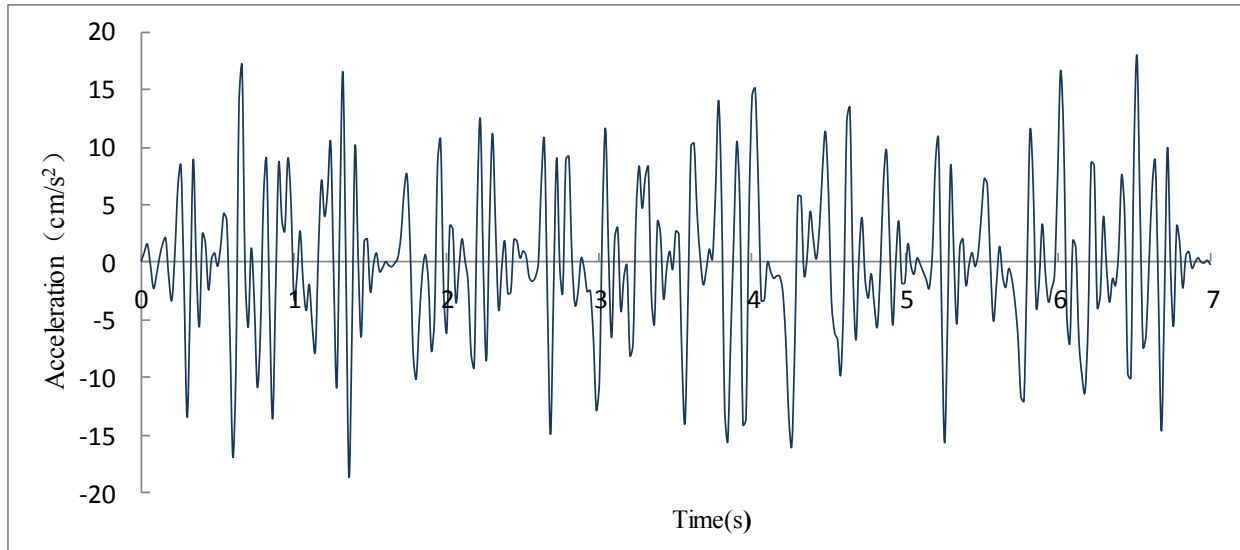


Fig. 2. Time-history curve of the acceleration speed of the seismic wave reduced to earthquake intensity IV

Table 1. Physical and mechanical properties of the rock layer

Item	Density / kg·m ⁻³	Cohesion /MPa	Tensile Strength /MPa	Internal Friction Angle /°	Young's Modulus /GPa	Poisson's ratio
Limestone	2600	1	0.6	40	25	0.22

Table 2. Physical and mechanical properties of the structural planes

Item	Density /kg·m ⁻³	Cohesion /MPa	Tensile Strength /MPa	Normal Stiffness /GPa·m ⁻¹	Tangential Stiffness /GPa·m ⁻¹
Bedding plane	0.030	0.08	32	10.2	6.4
Rear splay fracture	0.006	0.003	20	8.2	5.1

With the characteristics of the bedding rock slope and dynamic loading taken into consideration, a determination method for the limit equilibrium state of the slope is proposed, in which the trend of the time-history curve of the key point displacement is used to determine whether the slope remains stable or not. The specific determination process is as follows:

The main criterion for the stable state of the slope is that the time-history curve of the key point displacement tends to converge along the latter time axis, which means the displacement does no change with time in such period. Similarly, the proof for the slope being instable is that the time-history curve of the key point displacement is inclined to diverge along the latter time axis, in which case the key

point displacement keeps changing in such period. Taking the case of the rock slope with the rear splay fracture and continuous structural plane as an example, the horizontal permanent displacement change rate slightly increases with the growing reduction factor when the reduction factor is below 1.14. However, with the reduction factor beyond 1.14, the change rate of the horizontal permanent displacement grows significantly with the increase in the reduction factor (see Fig. 3). Thus, it is safe to say that with K=1.14, the slope reaches its critical stable state under the dynamic loading of earthquake intensity V. In other words, a reduction factor of 1.14 can be regarded as the dynamic safety factor for the slope under earthquake intensity V.

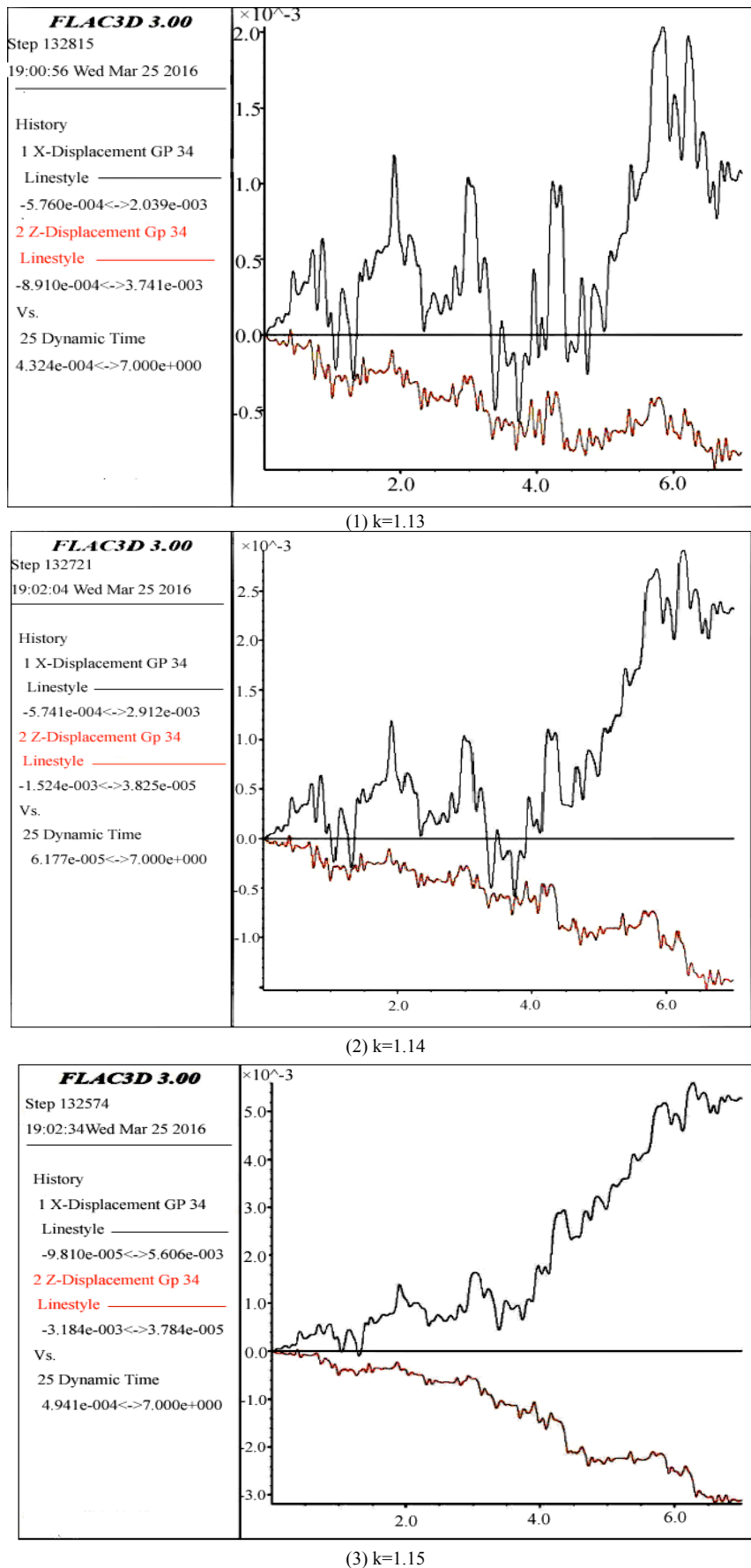


Fig. 3. Time-history curve of the horizontal displacement of the observation point

The safety factor of the described slope under the pseudo-static dynamic loading is analyzed using the limit equilibrium method to validate the calculation results from

the displacement vector diagram method used in this paper. The calculation model is the same as the one used by FLAC^{3D}. The pseudo-static dynamic loading is defined as

equal to earthquake intensity IV and the acceleration velocity is 0.022 g. The loading is evenly distributed along the slope, and the synthetic affection coefficient is 0.23. The calculated safety factor from the limit equilibrium method is 1.06. By comparing the results of the two methods, it can be observed that the safety factors are slightly different in magnitudes and generally close to each other, with a gap of only 7%. The difference can be attributed to the different dynamic loading inputs. In the finite difference method, the loading is represented by the applied stress time-history curve on the slope bottom, whereas in the limit equilibrium method, the loading input is constant and pseudo-static. Meanwhile, the sliding surfaces determined by the two methods both coincide with the structural plane penetrating through the slope. The safety factors and basically consistent sliding surfaces indicate the validity of the displacement vector diagram method used in this paper. Hence, analyzing the slope safety factors under dynamic loading using FLAC^{3D} is possible.

As shown in the previous case study of the dynamic strength reduction method, the permanent displacement of the potential sliding body basically changes in a small range after a one-time earthquake shock when the rock mass remains stable. In other words, the displacement time-history curve converges. In comparison, if the rock mass is unstable, after just one shock, the permanent displacement dramatically increases together with a significant growth in the change rate, indicating that the displacement time-history curve diverges. Therefore, under a frequently-occurring micro seismic wave, the dynamic stability of the bedding rock slope can be determined by the convergence of the slope displacement time-history curve. To identify the critical state of the slope accurately, the horizontal displacement difference between observation points on the slope surface and the rock base can be taken as the stability criterion.

The failure pattern for the bedding rock slope is mainly sliding along the bedding plane or the weak plane inside the rock mass, and sudden changes occur in the displacements of the rock layers above and below the sliding surface. Therefore, the potential sliding surface among the many bedding planes can be identified in the horizontal displacement contour map.

Table 3. Physical and mechanical properties of the rock

Item	Internal Friction Angle /°	Cohesion /MPa	Density /kg·m ⁻³	Bulk Modulus /GPa	Shear Modulus /GPa	Tensile Strength /MPa
Metamorphic Tectonite	38	1.0	2500	5.556	4.167	0.7

Table 4. Physical and mechanical properties of the structural plane

Item	Cohesion /MPa	Normal Stiffness /GPa·m ⁻¹	Tangential Stiffness /GPa·m ⁻¹	Tensile Strength /MPa
30	30	12.4	8.6	10

The cosine shear wave is used as the input wave of the dynamic loading. The time-history curve of the acceleration speed is $a = \lambda \cos(2\pi ft)$, in which equation λ is equal to 0.22m/s² (of earthquake intensity IV). The input of seismic wave still needs to be transformed into the corresponding stress time-history.

The viscous boundary available in FLAC^{3D} is used to absorb the energy of the incident waves and minimize the effect of boundary-reflected waves under dynamic loading. The input of dynamic loading should be in the form of stress

4.2 Case 2

Based on the analysis in the previous section, the factors that affect the safety of the bedding rock slope, such as the slope height, slope gradient, bedding inclination angle, and loading frequency, are studied in this section in a single-factor manner using FLAC^{3D}.

The calculation model is shown in Fig. 4. The rock slope contains a group of beddings with an average thickness of 10 m unless stated otherwise. For the model geometry, the horizontal section length of the slope toe is 1.5 times the slope height whereas the horizontal section length of the slope top is 2.5 times the slope height. The slope angle is defined as α , the bedding inclination angle β , and the slope height H. The element size of the model meets the requirements to avoid distortion of the seismic waves in the analysis.

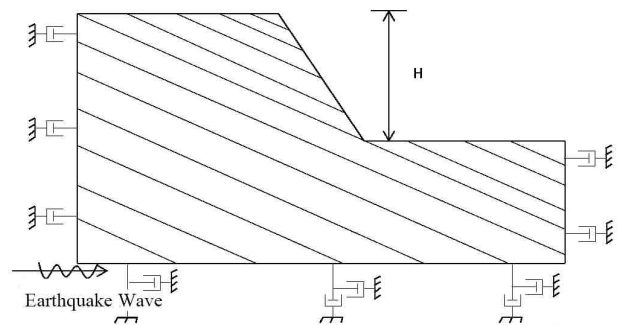


Fig. 4. Analysis model geometry and boundary condition

In the simulation, the rock is considered the ideal elastic-plastic material, and the Mohr-Coulomb strength criterion is used as the yield criterion. The Coulomb's sliding model with face contact is used, with regard to the bedding plane [18]. The physical and mechanical properties of the rock layer and the structural plane referring to other similar engineering are shown in Table 3 and Table 4, respectively [19].

time-history curve, and the transformation equations from the velocity time-history curve to the stress time-history are as follows:

$$\sigma_n = -2(\rho C_p) v_n \tag{4}$$

$$\sigma_s = -2(\rho C_s) v_s \tag{5}$$

where

σ_n = normal stress;

σ_s = shear stress;

ρ = media density;

C_p , C_s are the travelling speeds of the P and S waves in the media, respectively; and,

v_n , v_s are the speeds in the vertical and horizontal directions, respectively.

The local damping is used in the simulation, and the corresponding damping coefficient is assumed to be 0.15 according to Deng Y. R [18].

4.2.1 Effects of the slope height on the safety factors

Five different scenarios of the slope height are used for the analysis, namely, the slope heights of 60, 100, 150, 200, and 300 m. The slope angle α is equal to 60° . The bedding inclination angle β is equal to 20° . The seismic wave frequency f is equal to 3Hz. The horizontal displacement difference of the observation points is shown in Fig. 5. The horizontal displacement contour map is shown in Fig. 6.

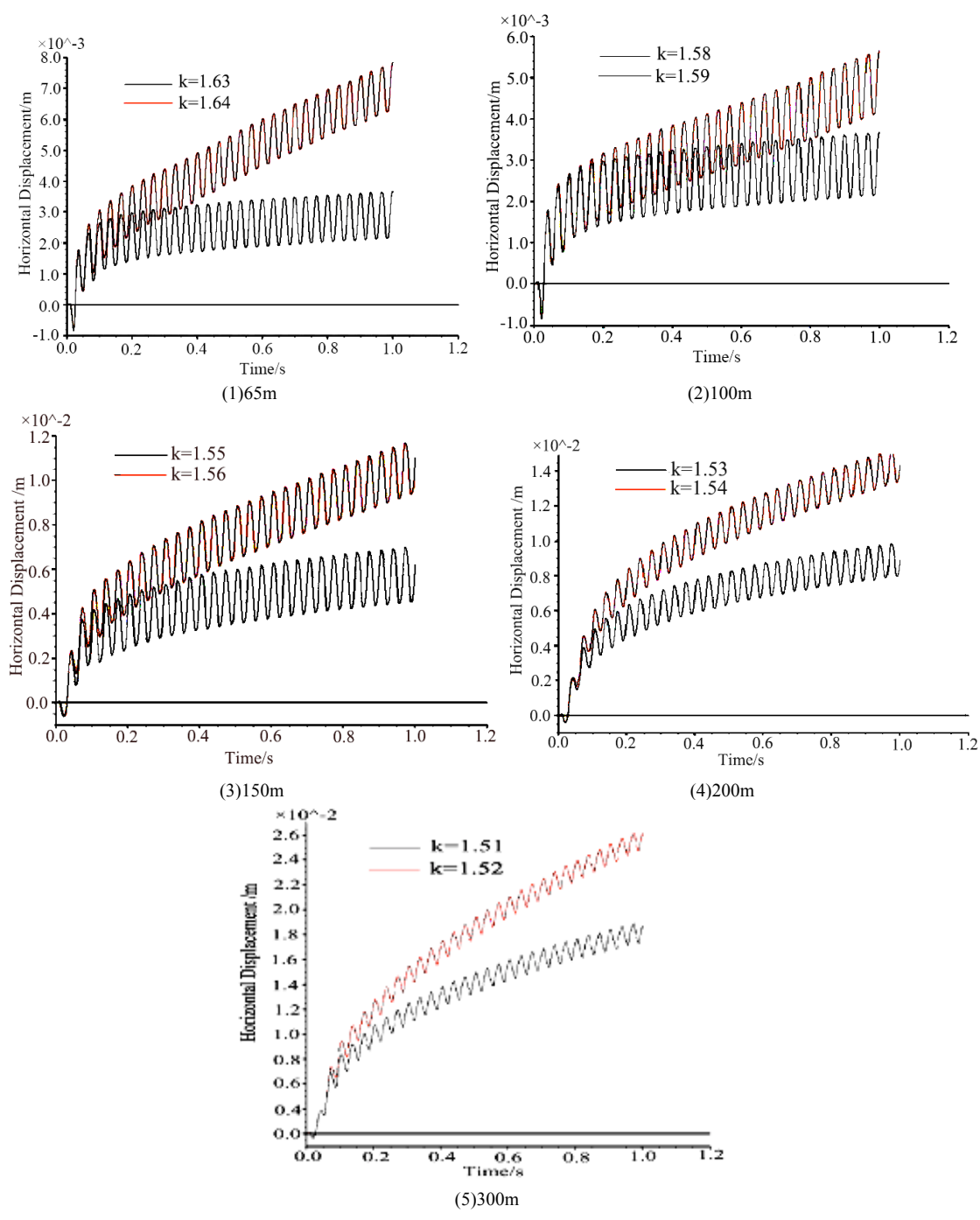
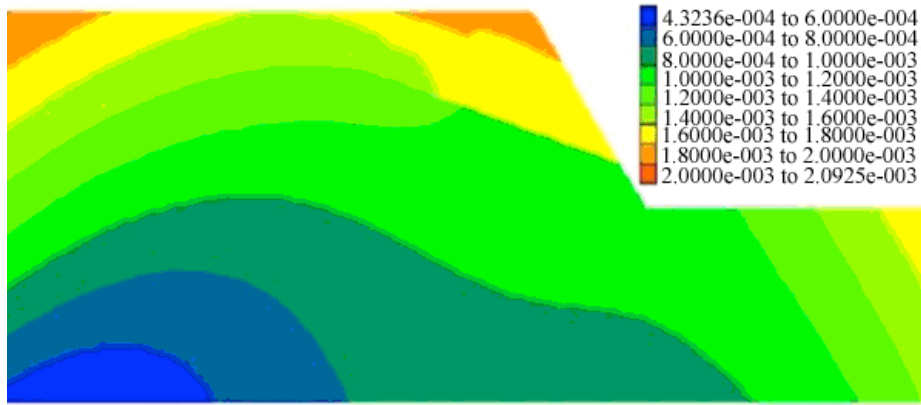
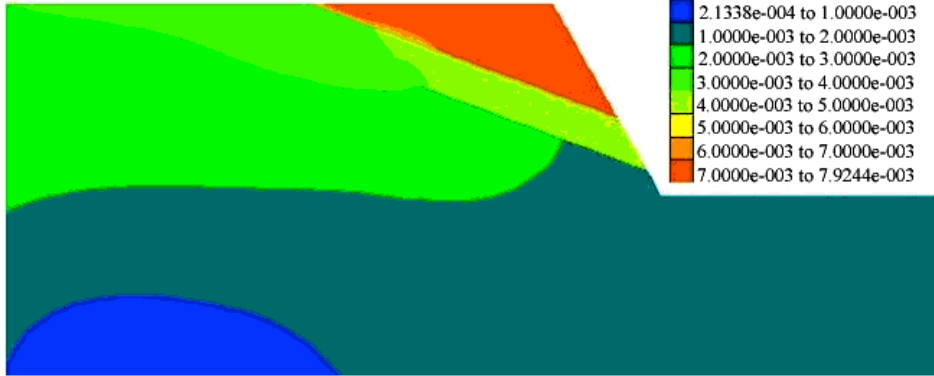


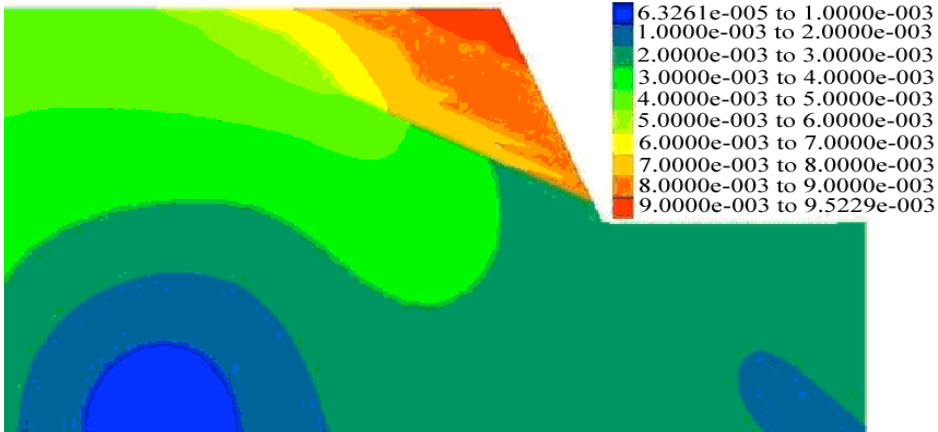
Fig. 5. Horizontal displacement difference between the slope top and base rock with different slope heights ($f = 3\text{Hz}$, $\alpha = 60^\circ$, $\beta = 20^\circ$)



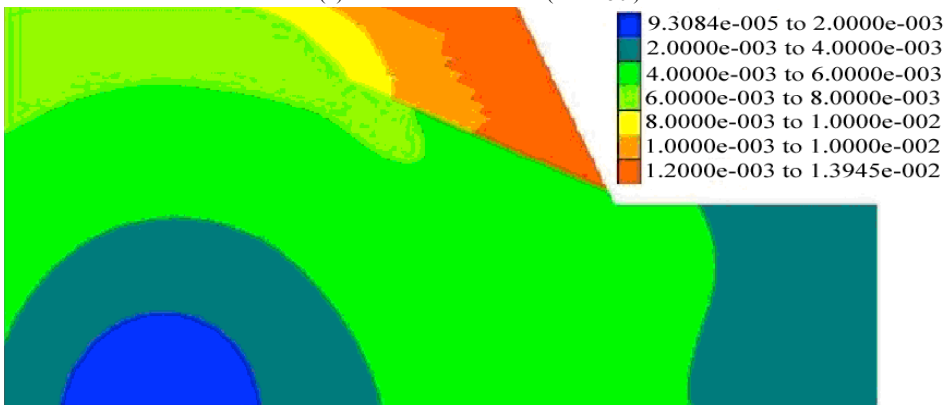
(1) Reduction factor=1.63 ($H = 60$)



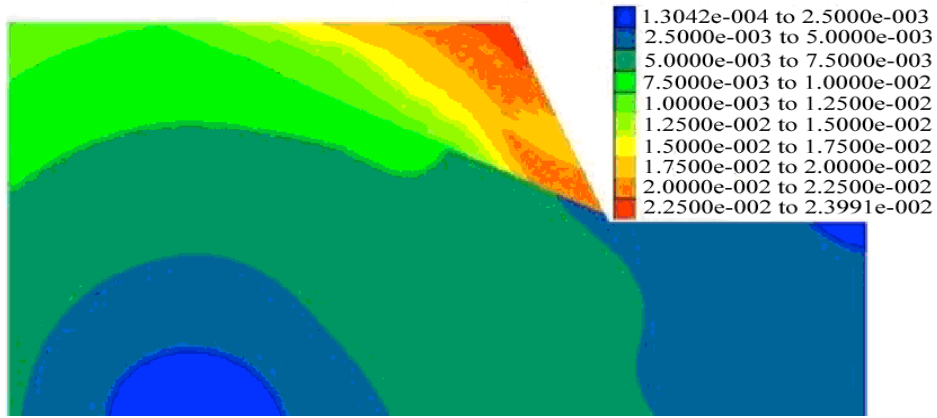
(2) Reduction factor=1.57 ($H = 100$)



(3) Reduction factor=1.55 ($H = 150$)



(4) Reduction factor=1.53 ($H = 200$)



(5) Reduction factor=1.51 ($H = 300$)

Fig. 6. Contour map of the displacement in the X direction (m)

The relationship between slope height and dynamic safety factors is shown in Fig. 7. The dynamic safety factors gradually decrease with the increase in the slope height. At a slope height range of 0 to 150 m, the safety factors decrease relatively fast with slope height variation, indicating a high sensitivity of the safety factors to the variation at the slope height range of 0 to 150m, and slow change in the safety factors in the range of 150 to 300 m.

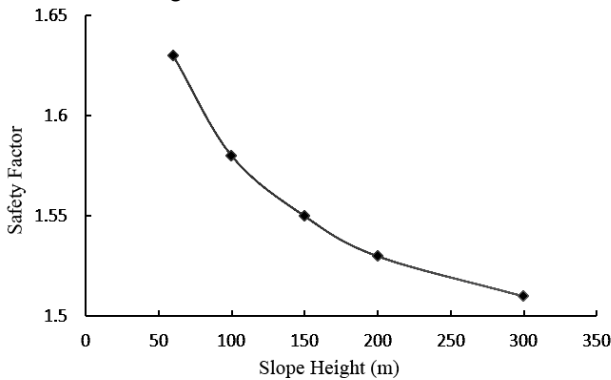
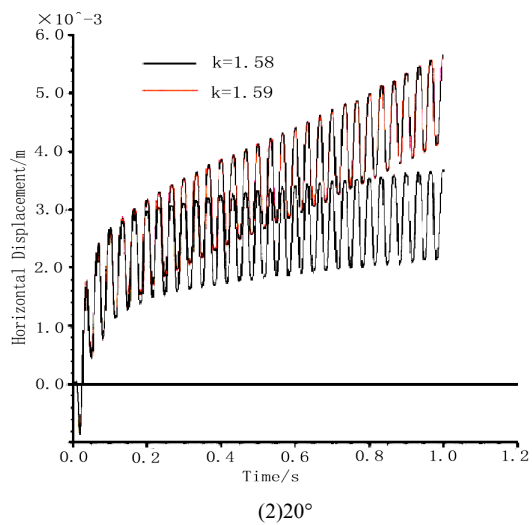
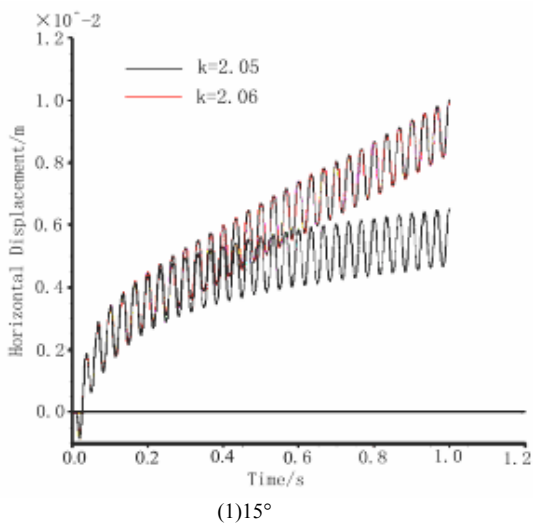


Fig. 7. Slope height vs. safety factors ($f = 3Hz, \alpha = 60^\circ, \beta = 20^\circ$)

4.2.2 Effects of the bedding inclination angle on the safety factors

Five different bedding inclination angle scenarios are used to analyze the effects of the bedding inclination angle on the stability of the bedding rock slope, namely, bedding inclination angles of 15°, 20°, 25°, 30°, and 35°. Slope angle $\alpha = 60^\circ$ is equal to 60°. The slope height $H = 100m$ is equal to 100 m. The seismic wave frequency $f = 3Hz$ is equal to 3Hz. The horizontal displacement difference of the observation points is shown in Fig. 7. The horizontal displacement contour map is shown in Fig. 8.

The relationship between the safety factors of the rock slope and the bedding inclination angle is shown in Fig. 9. As shown in the figure, the dynamic safety factors reduce significantly with the increase of bedding inclination angle. The change magnitude is relatively large, indicating that the bedding inclination angle has direct effects on the stability of the bedding rock slope.



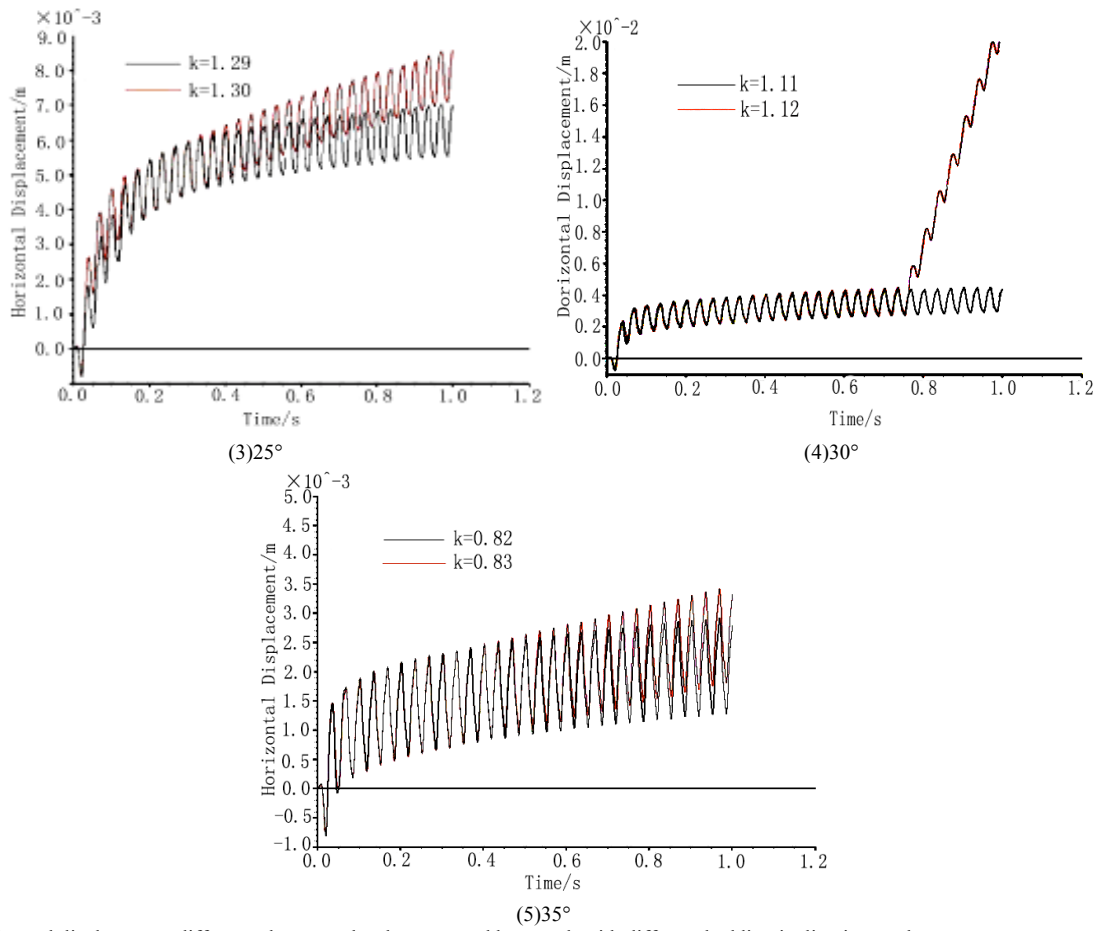
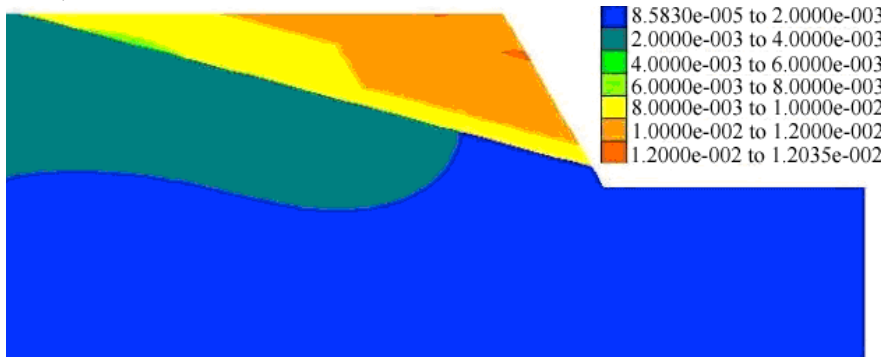
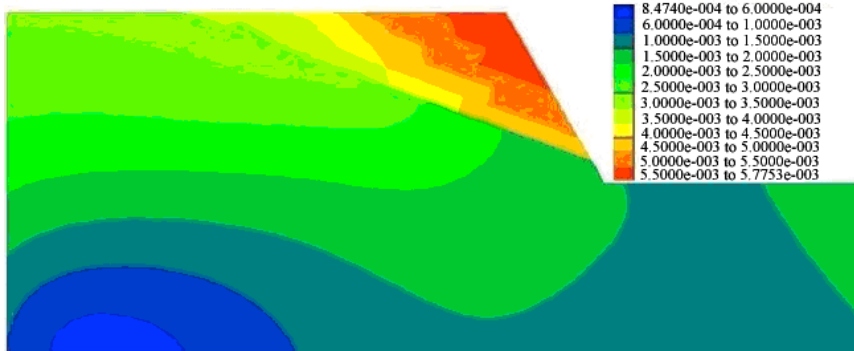


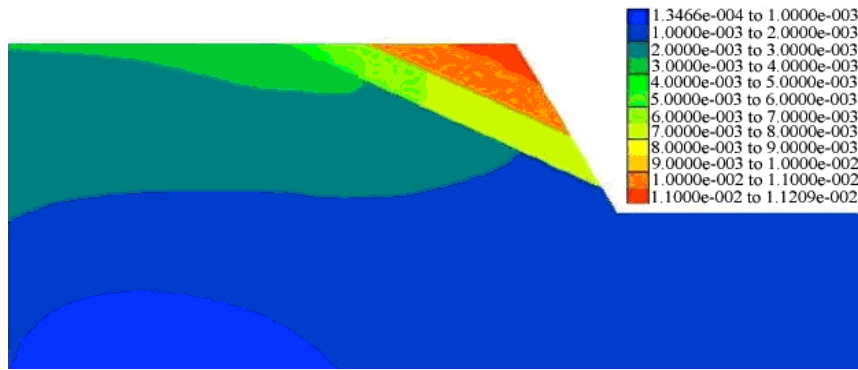
Fig. 8. Horizontal displacement difference between the slope top and base rock with different bedding inclination angles ($f = 3\text{Hz}, \alpha = 60^\circ, H = 100\text{m}$)



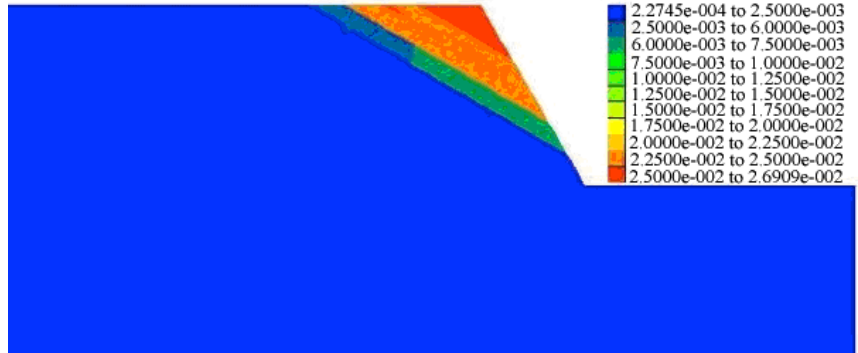
(1) Reduction factor=2.06 ($\beta = 15^\circ$)



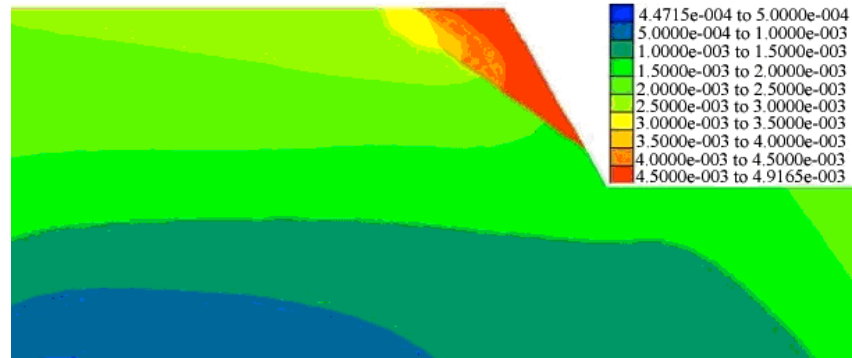
(2) Reduction factor=1.58 ($\beta = 20^\circ$)



(3) Reduction factor=1.30 ($\beta = 25^\circ$)



(4) Reduction factor=1.12 ($\beta = 30^\circ$)



(5) Reduction factor=0.82 ($\beta = 35^\circ$)

Fig. 9. Contour map of the displacement in the X direction (m)

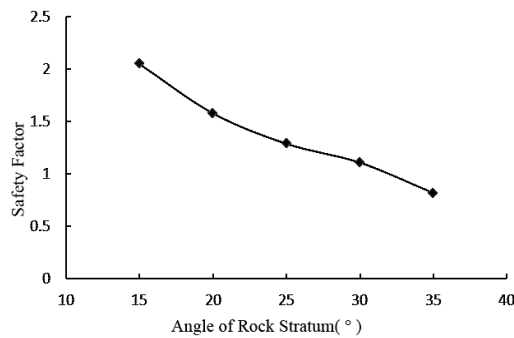


Fig. 10. Bedding inclination angle vs. safety factors ($f = 3\text{Hz}$, $\alpha = 60^\circ$, $H = 100\text{m}$)

4.2.3 Effects of the slope angle on the safety factors

Five cases, with slope angles of 45° , 50° , 55° , 60° , and 70° , are established to study the effects of the slope angle on the stability of bedding rock slope. Bedding inclination angle β is equal to 20° . Slope height H is equal to 100m . The seismic wave frequency f is equal to 3Hz . The horizontal displacement difference of the observation points is shown in Fig. 11.

The horizontal displacement contour map with different slope angles is shown in Fig. 12, which shows that the potential sliding surfaces under the 3-Hz seismic wave are basically similar to each other.

The correlation between the slope angle and the dynamic safety factors is shown in Fig. 13. As shown in the figure, at a slope angle range of 45° to 55° , the dynamic safety factors decrease with growth in the slope angle; in the range of 55°

to 70° , the dynamic safety factor tends to reach its stable state and the change magnitude is relatively small.

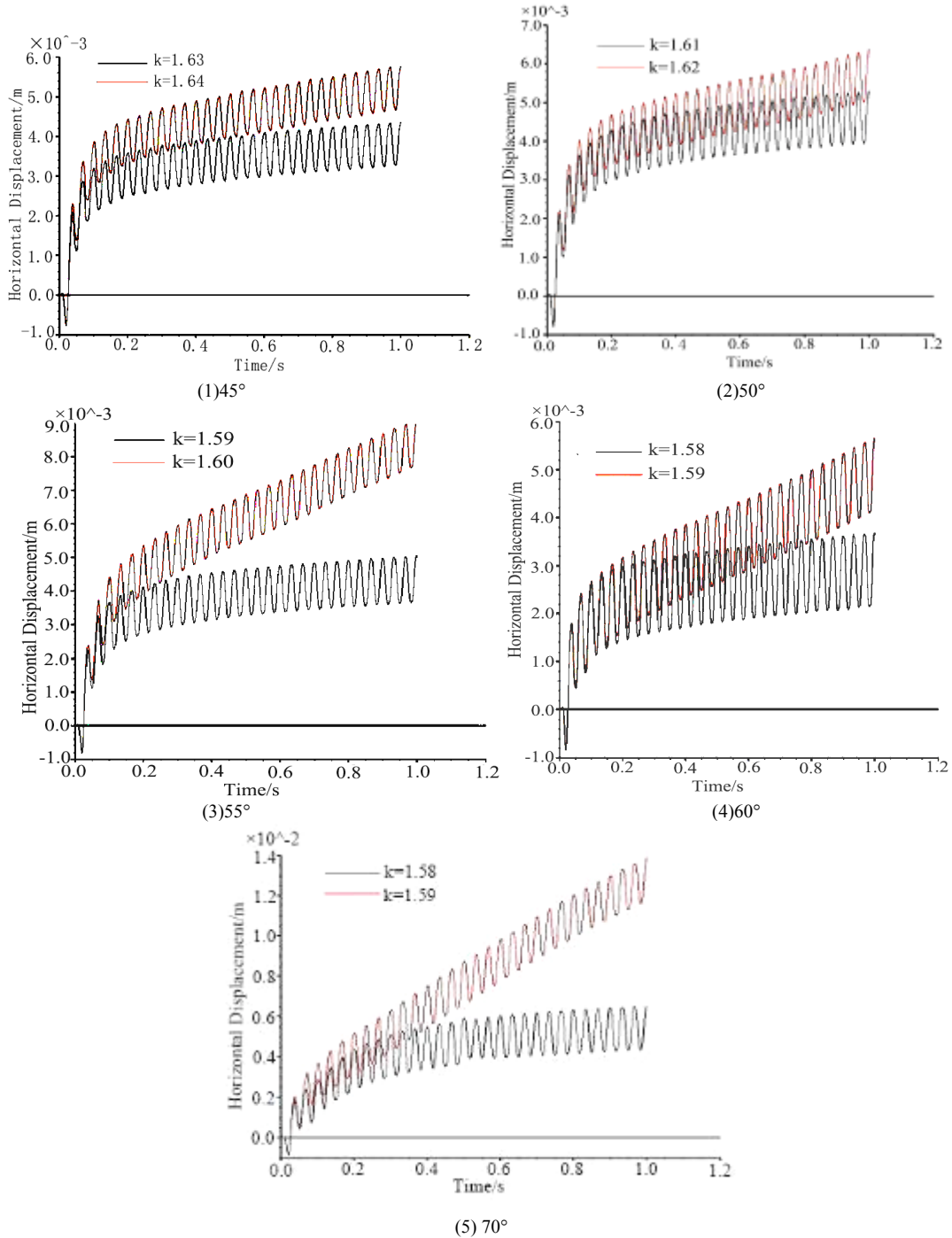
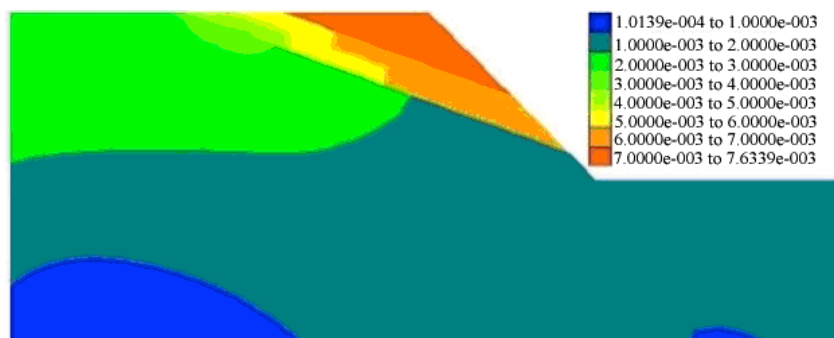
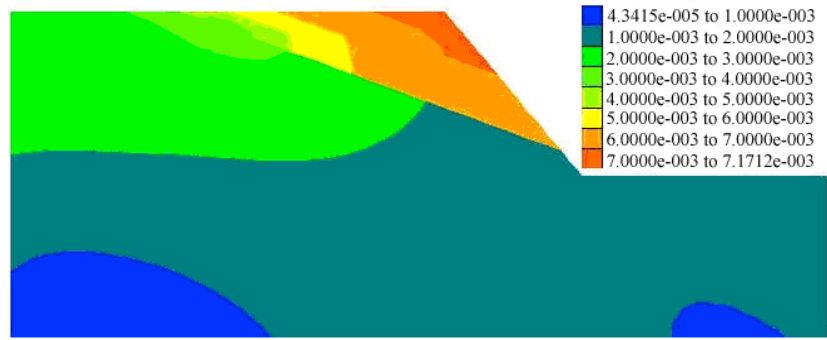


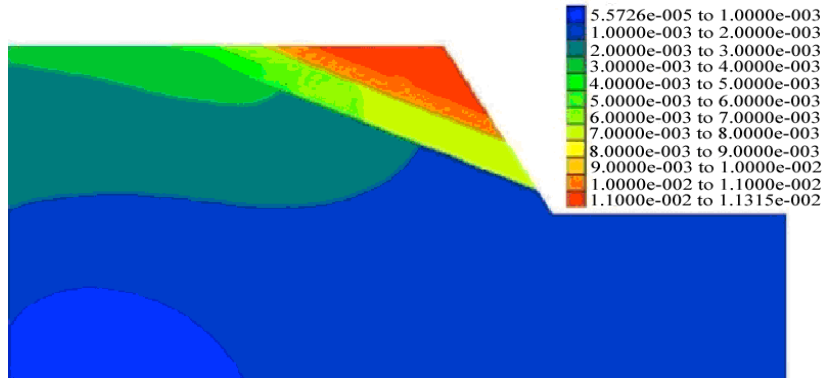
Fig. 11. Horizontal displacement difference between the slope top and base rock with different slope angles ($f = 3\text{Hz}$, $\beta = 20^\circ$, $H = 100\text{m}$)



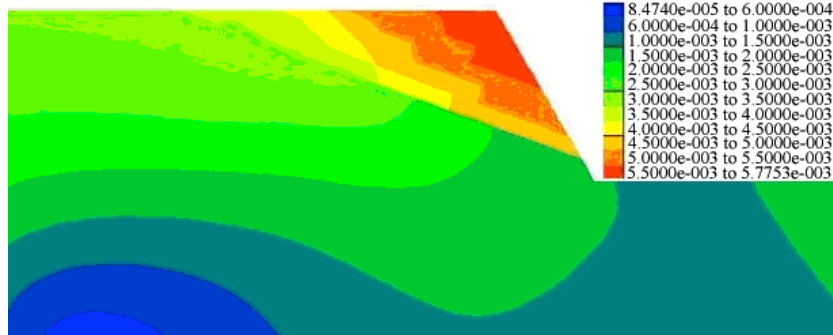
(1) Reduction factor=1.64 ($\alpha = 45^\circ$)



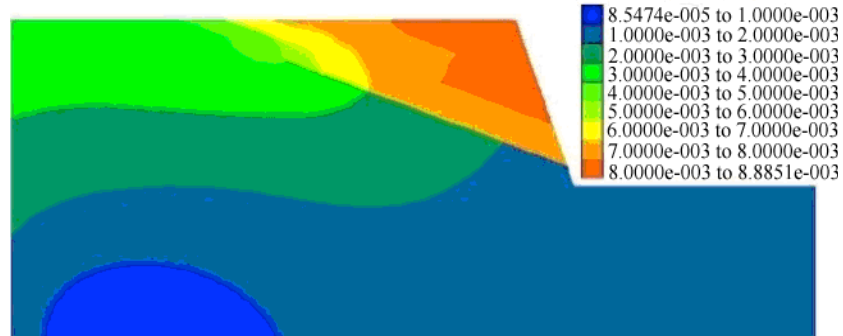
(2) Reduction factor=1.60 ($\alpha = 50^\circ$)



(3) Reduction factor=1.60 ($\alpha = 55^\circ$)



(4) Reduction factor=1.58 ($\alpha = 60^\circ$)



(5) Reduction factor=1.58 ($\alpha = 70^\circ$)

Fig. 12. Nephogram of X direction displacement (m)

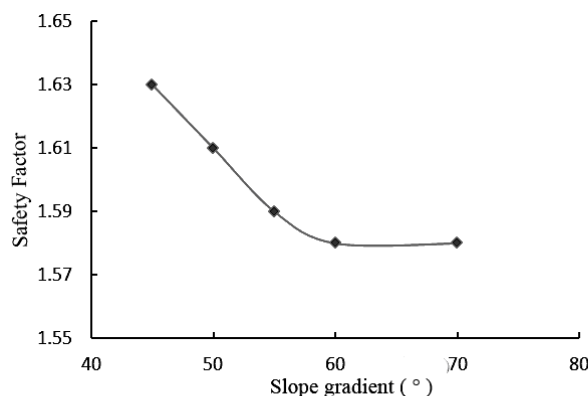


Fig. 13. Relation between slope gradient and safety factor ($f = 3\text{Hz}$, $\beta = 20^\circ$, $H = 100\text{m}$)

5 Conclusions

The dynamic response and deformation process of the rock slope-containing surface under the dynamic loading was studied using method of estimating the critical state of the bedding rock slope using the trend of the key point displacement time-history curve. The corresponding safety factor and sliding surface were then obtained. Analyses on the effects of the slope height, slope gradient, and bedding inclination on the safety factors of the bedding rock slope were also studied. The conclusions are obtained as follows.

(1) Results of safety factor and sliding surface calculated via the introduced method were compared with those from the limit equilibrium method. The comparison showed that the difference between the two safety factors was small and the sliding surface locations were basically consistent, which successfully validated the method used in this paper.

(2) In general, the dynamic stability of the bedding rock slope was gradually compromised by the increasing slope height. At the slope height range of 0 to 150 m, the safety factors changed relatively fast as the slope height varied, whereas in the range of 150 to 300 m, the change was slow.

(3) The dynamic safety factors of the slope significantly decreased with the growth of the bedding inclination angle.

(4) A transformation of the change pattern of dynamic slope safety factors from the quick to the slow mode was also observed as the slope angle varied. When the slope angle lay at the 45° to 55° , the dynamic safety factors decreased with the growing slope angle; at a slope angle of 55° to 70° , the slope safety factor approached the stable state.

Rock slope stability was studied in this paper. However, given the complexity of the problem, further studies are necessary to determine the effects of structural face interval, seismic wave amplitude, and frequency on the safety factors of bedding rock slope under dynamic loading, as well as the consistency of the theoretical solution and numerical solution for the safety factor of a bedding rock slope.

Acknowledgements

This work was supported by “the National Natural Science Foundation of China (No. 41372356)”, “2015 Chongqing University Postgraduates’ Innovation Project” and “the Fundamental Research Funds for the Central Universities of China (No. 106112014CDJZR200008)”.

References

- Dai, F. C., Xu, C., & Yao X., et al. “Spatial Distribution of Landslides Triggered by the 2008 Ms 8.0 Wenchuan Earthquake, China”. *Journal of Asian Earth Sciences*, 40(4), 2011, pp.883 -895.
- Bommer, J. J., & Rdr G., C. E., “Earthquake-induced Landslides in Central America”. *Engineering Geology*, 63(3), 2002, pp. 189-220.
- Randall, W. J., “Methods for assessing the stability of slopes during earthquakes-A retrospective”. *Engineering Geology*, 122(1-2), 2011, pp.43-50.
- Shukla, S. K., & Hossain, M. M., “Stability analysis of multi-directional anchored rock slope subjected to surcharge and seismic loads”. *Soil Dynamics and Earthquake Engineering*, 31(5), 2011, pp.841-844.
- Tian, X.F., Sun, J.Z., Liu Y.Q., & Jia L., et al. “Critical acceleration analysis of slope earthquake stability”. *Science Technology and Engineering*, 12(23), 2012, pp.5807-5811
- Sun, J.Z., Zhao, T., & Li, G., et al. “Load increasing method for analysis of slope earthquake stability”. *Journal of Engineering Geology*, 20(5), 2012, pp.751-759
- Zhao, T., Sun, J.Z., & Zhang, B., et al. “Analysis of slope stability with dynamic overloading from earthquake”. *Journal of Earth Science*, 23(3), 2012, pp.285-296.
- Newmark, N. M., “Effects of earthquakes on dams and embankments”. *Geotechnique*, 15(2), 1965, pp.139-160.
- L Scholtès, Frédéric-Victor Donzé. “Modelling progressive failure in fractured rock masses using a 3D discrete element method”. *International Journal of Rock Mechanics & Mining Sciences*, 52(6), 2012, pp.18-30.
- Zhang, Y.B., Chen, G.Q., & Zheng, L., et al. “Effects of geometries on three-dimensional slope stability”. *Canadian Geotechnical Journal*, 50(3), 2013, pp.233-249.
- Guo, M. W., Ge X. R., & Wang, S. L., “Slope stability analysis under seismic load by vector sum analysis method”. *Journal of Rock Mechanics and Geotechnical Engineering*, 3(3), 2011, pp.282-288.
- Bhasin, R., Kaynia, A. M., “Static and dynamic simulation of a 700-m high rock slope in Western Norway”. *Engineering Geology*, 71(3-4), 2004, pp. 213 -226.
- Teng, G. L., Chen, Y. M., Shi, Y.C., Sun, C.S., Lu, Y. X., & Qiang, Z. Y., “A study on the influencing factors of joint rock slope stability under earthquake activity”. *China Earthquake Engineering Journal*, 35(1), 2013, pp.119-125.
- Facciorusso, J., Madiari, C., & Vannucchi, G., “A grade-3 method of zonation for seismic slope stability: An Italian case study”. *Soil Dynamics and Earthquake Engineering*, 36 (4), 2012, pp.96-110.
- Zheng, Y. R., Ye, H. L., & Huang R.Q., “Analysis and discussion of failure mechanism and fracture surface of slope under earthquake”. *Chinese Journal of Rock Mechanics and Engineering*, 28(8), 2009, pp.1714-1723.
- Locat, A., Leroueil, S., & Fortin, A., et al. “The 1994 landslide at Sainte-Monique, Quebec: geotechnical investigation and application of progressive failure analysis”. *Canadian Geotechnical Journal*, 52(4), 2014, pp.1-15
- Chen, X.P., Huang, J.W., Yin, S.H., & Zheng, J.Z., et al. “Experimental study of strength property of slip zone soils”. *Rock and Soil Mechanics*, 32(11), 2011, pp.3212-3218.

18. Itasca Consulting Group Inc., “*UDEC (universal distinct element code) user's manual (version3.0)*”. Minneapolis: Itasca Consulting Group Inc., 1996.
19. Stianson, J. R., Fredlund, D. G., & Chan, D., “Three-dimensional slope stability based on stresses from a stress-deformation analysis”. *Canadian Geotechnical Journal*, 48(6), 2011, pp.891-904